Developments on using supercontinuum sources for high resolution multi-imaging instruments for biomedical applications

Gianni Nteroli[a], Magalie Bondu[b], Peter M. Moselund[b], Adrian Podoleanu[a] and Adrian Bradu[a]
[a]Applied Optics Group, School of Physical Sciences, University of Kent, Canterbury, UK
[b]NKT Photonics A/S, Blokken 84, Birkeroed, Denmark, 3460

ABSTRACT

We report on further progress made on enhancing the capabilities of a multi-imaging modality instrument capable of producing high resolution images of biological tissues. At the core of the instrument is a supercontinuum (SC) source. Two SC sources commercialized by NKT Photonics were employed for our experiments: SuperK COMPACT and SuperK Extreme (EXR9). Using these two sources, we assembled an instrument capable to simultaneously provide in real-time cross-section high-resolution Optical Coherence Tomography (OCT) and Photo-acoustic (PA) images in various spectral ranges. Currently, the OCT channel is operating in the IR range around 1300 nm to allow better penetration into the tissue using either the COMPACT or the EXR9. The measured optical power on the sample is in both cases above 9.5 mW. An *in-house* spectrometer equipped with a sensitive InGaAs camera capable of operating at 47 kHz and sampling data over a spectral range from 1205 to 1395 nm was developed. A constant axial resolution provided by the instrument in the OCT channel over a range of 1.5 mm was experimentally measured (4.96 µm), matching the theoretical prediction. The spectral range 500-800 nm was used for PA channel. The COMPACT, used in the PA channel, can select the central wavelength and the spectral bandwidth of operations. Typically, the optical energy per pulse on the sample is superior to 60 nJ when a bandwidth superior to 50 nm is employed. This make the instrument usable for PA imaging of tissues.

Keywords: optical coherence tomography, photo-acoustics, high-resolution, multi-spectral imaging, multi-imaging.

1. INTRODUCTION

Optical Coherence Tomography is a high-resolution imaging technique able to measure backscattered light wave-fronts generated from a low-coherence light source illuminating the sample [1]. The axial resolution of OCT ranges typically from one micron to tens of microns and an axial range in tissue limited to only 1-1.5 mm, depending on various parameters such the central wavelength, the spectral bandwidth, optical power on the sample, etc. So far, OCT systems have been used to image a variety of tissues *in-vivo* or *ex-vivo* that can be accessed either directly or via endoscopes or catheters, including the eye. To further extend the limited axial resolution provided by the OCT instruments, PA imaging was proposed as an emerging biomedical imaging technique capable of providing optical absorption contrast at an acceptable axial resolution [2]. An ultrasonic transducer is employed to measure the ultrasonic waves generated through the photoacoustic effect, which generates a transient temperature rise due to the short pulse light absorption in the biological tissue. The produced ultrasonic waves are used to reconstruct the light absorption distribution which directly can be related for example to the vasculature of tumors [3]. Then, using multispectral PA techniques, the PA signals can be used to look at cell oxygenation, so indicators of tumor metabolism and therapeutic response become available.

Multimodal imaging modalities show great promise, providing complementary information and diverse contrast of biological tissues. In all the previous reports, each imaging modality benefited from its own optical source. This indicates a high cost of the instrument as well as restrictions in the operation of the instrument to spectral ranges determined by the optical source employed. In a recent report, we demonstrated that by using a single SC (SuperK COMPACT) decent quality images in terms of signal-to-noise ratio can be obtained in both channels, OCT and PA [4]. Here, we report further development on this research activity, especially on enhancing the axial resolution and the sensitivity in the OCT channel by designing a new spectrometer and on taking different approach on illuminating the sample to enhance the energy per pulse and thus the signal-to-noise ratio in the PA channel.

2. EXPERIMENTAL SET-UP

Set-up 1 (a single supercontinuum source for both imaging modalities). The multi-imaging modality experimental setup is depicted on the right side of Fig. 1. Light from the SuperK COMPACT is conveyed towards the dual band filter (Varia, NKT Photonics A/S) which splits the spectrum into two spectral bands: a short wavelength, covering all the VIS

range, ranging between 450 and 850 nm, and a longer wavelength band in the IR, around 1300 nm. The short wavelength band is used for PA. At a later stage, this band will also be used to deliver light for a VIS OCT instrument. Currently only the IR OCT channel is operational. In the IR OCT channel light from Varia is split by the 50/50 broadband directional fiber coupler towards a reference arm and a sample arm. Light from both outputs of the filter are multiplexed using a dichroic filter D and conveyed towards the sample to be investigated via a galvo-scanner head GXY and a microscope objective (Mitutoyo MPlan NIR 10). To maximize the power on the sample for PA, we did not convey light via optical fibers. A transducer needle TN based on a PMN-PT crystal is immersed into the aqueous close to the sample. The TN converts the US wave into an electric signal which is amplified before digitization. The digitization is performed in synchronism with the pulse repetition frequency of the SC which is around 20 kHz.

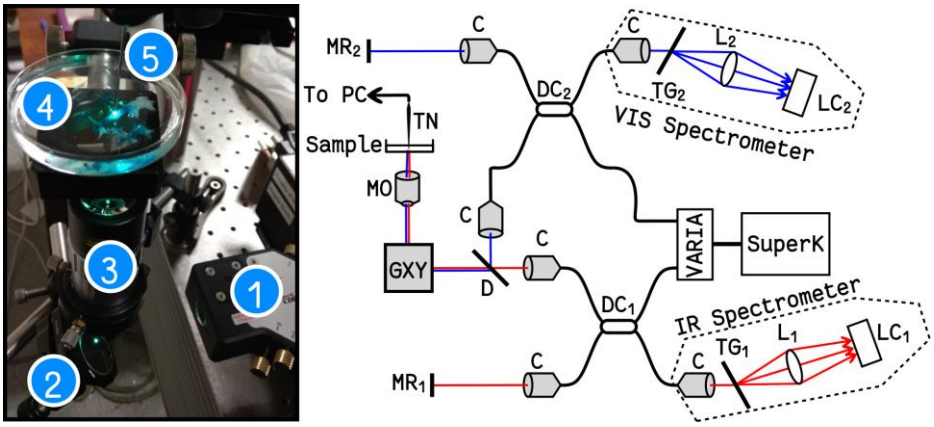

Figure 1: Schematic diagram of the instrument (left) and a picture showing the arrangements in the sample arm (right). C: parabolic collimators; $L_{1,2}$: achromatic lenses; $LC_{1,2}$: linear cameras; $TG_{1,2}$: transmission diffraction gratings; $DC_{1,2}$: directional couples; MO: microscope objective; GXY: orthogonal galvo-scanners; $MR_{1,2}$: flat mirrors; TN: needle transducer. In the left image, 1: Varia's VIS output; 2: flat mirror; 3: microscope objective; 4: sample; 5: transducer.

IR light backscattered by the sample interferes with light originating from the reference arm (back-reflected by MR1), at DC_1. To detect the channel spectra, the IR Spectrometer whose sketch is presented in Fig. 1 was devised. It incorporates a transmission diffraction grating TG_1 (Wasatch Photonics, model HP 1145 l/mm blazed @ 1310 nm) an achromatic doublet pair lens L_1 (Thorlabs, AC508-150-C). A linear camera (LC1, Goodrich, model SU1014-LDHI.7RT-0500/L) equipped with 1024 pixels is used to read the channeled spectra synchronous with the repetition rate of SuperK. At a later stage, a VIS spectrometer will be ensembled. For this one we are intending to use a linear camera LC_2 (Basler, spL4096-140km), whose reading will also be synchronized with the SC source.

Set-up 2 (two supercontinuum sources employed). The schematic diagram of this instrument is depicted in Fig. 2. The PA channel still uses the SuperK Compact, however the OCT channel uses the EXR9. The spectrometer used was identical to the one presented in Fig. 1. Now, the synchronization between the camera reading and the optical pulses generated by EXR9 is not possible anymore. This allows in principle to take advantage of the full speed of the camera employed (47 kHz) to produce B-scan OCT images faster by at least a factor of 2 than the PA B-scan images.

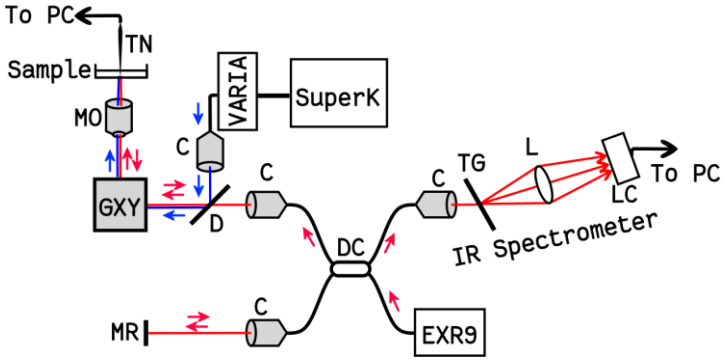

Figure 2: Schematic diagram of the instrument 2 employing two SCs). C: parabolic collimators; $L_{1,2}$: achromatic lenses; LC: linear cameras; TG: transmission diffraction gratings; DC: directional couples; MO: microscope objective; GXY: orthogonal galvo-scanners; MR: flat mirrors; TN: needle transducer.

3. RESULTS AND DISCUSSION

The IR spectrometer was designed in such a way that a spectral bandwidth as wide as possible is accommodated by the 1024 pixels of the linear camera. As illustrated in Fig. 3(a), a quite good contrast was achieved over all the pixels the camera is equipped with (range of wavelengths from 1205 nm to 1395 nm (190 nm bandwidth) around a central wavelength of 1300 nm). Given that the shape of the spectrum as read by the camera is approximately Gaussian, with a full width at half maximum of around 150 nm, we can expect a theoretical axial resolution as good as 4.96 μm.

To correct for non-linearities, compensate for the dispersion left uncompensated in the interferometer which can be significant when using wide spectral bandwidths, and produce the sensitivity drop-off, we employed the Master-Slave technique [5-7]. By using it, we matched the theoretical values of the axial resolution over a quite large axial range (1.5 mm) as illustrated in Fig. 2(b). When spectra are subject to apodization, the axial resolution deteriorates to around 6.1 μm. The same axial resolutions were found for both supercontinuum sources, however EXR9 provides a sensitivity of at least 15 dB superior to that obtained with the COMPACT, for the same optical power on the sample, and the same reading speed of the camera (20 kHz).

The axial reflectivity profiles at various axial positions depicted in Fig. 3(b) were produced by windowing the theoretically inferred spectra using a Hamming filter. The apparent axial shift of maximum of sensitivity is an artifact due to high pass filtering of the channeled spectra employed to remove noisy low frequency components. Over the axial range of 1.5 mm, the sensitivity drops by around 8 dB. The sensitivity drop-off depicted in Fig. 3 was obtained using the COMPACT, however a similar one was achieved with the EXR9.

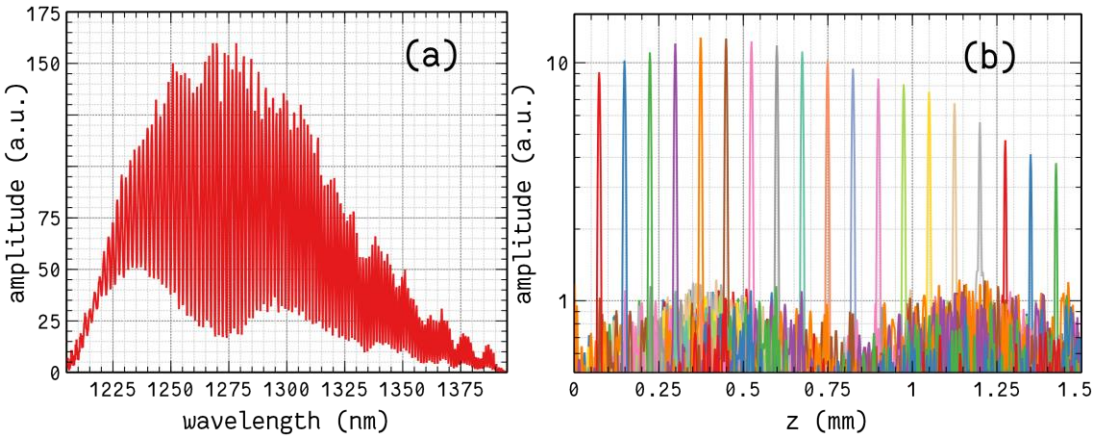

Figure 3: (a) Example of experimental channeled spectrum (z=0.5 mm) by LC_1 showing modulation over 190 nm. (b) Sensitivity roll-off of the OCT signal over 1.5 mm. Over this range the axial resolution exhibits quite low fluctuations. Data presented in this figure were generated using the COMPACT supercontinuum optical source. Similar plots could be generated using the EXR9, however the sensitivity of the instrument with EXR9 is better than that obtained when using the COMPACT by at least 15 dB for a given optical power on the sample.

To characterize the PA channel, we used a black duct tape immersed in water. We experimentally noticed that, for a given absorption of this sample, the response of the transducer TN scales linearly with the optical power on the sample. As illustrated in Fig. 4(d) the power on the sample increases with wavelength, however the amplitude of the PA signals decreases with wavelength for this particular sample. By doubling the spectral bandwidth, the power on the sample increases by a factor of 2. There is also a factor of 2 between the PA signals collected using the two spectral ranges.

To produce strong PA signals in biological tissues, the sources employed should provide an energy per pulse of over 50 nJ. The high repetition rate of the SC employed here (20 kHz), higher than those of the Q-switched lasers used for PA applications (typically tens of Hz) enables a greater number of pulses to be acquired and the signal to be averaged over a certain time. This offers the prospect of increasing the signal-to-noise ratio of the detected PA signal. Also, as we have the flexibility of manipulating the wavelength of the SC laser, we can adjust its operation to avoid undesirable absorption by various chromophores (as for example water absorption). For the experimental data presented in Fig. 4, at 500 nm, and a bandwidth of 50 nm, the average power measured on the sample was 1.2 mW, corresponding to an energy per pulse of 60 nJ which is enough for imaging biological tissues.

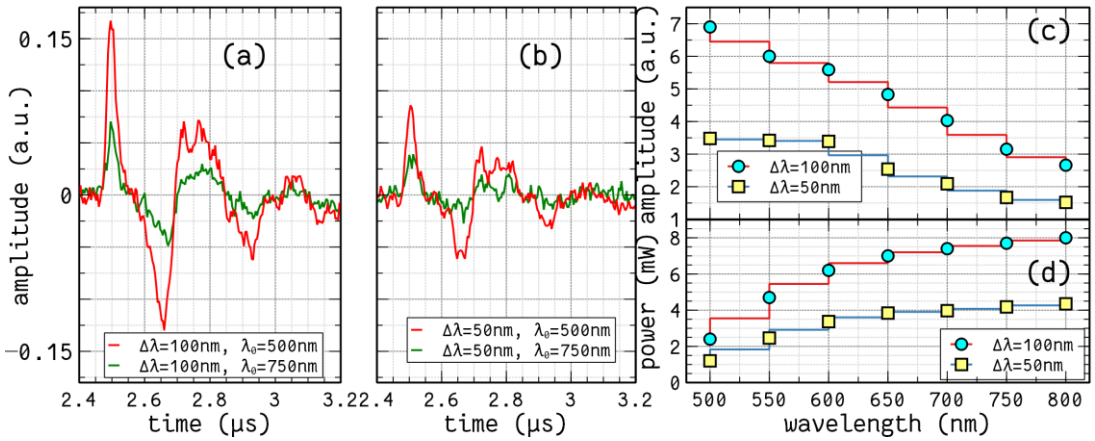

Figure 4: (a) and (b): typical PA signals for different wavelengths and bandwidths. (c) PA signals for several central wavelengths, computed by integrating signals as those depicted in (a) and (b). (d) Average power on the sample.

Using the instrument described above, OCT and PA images of various samples were produced. In Fig. 5(a-c), 3D OCT reconstructions of various samples are presented (thumb, tooth, finger). The measured axial resolution in these images is around 5 µm. Each volume has a size of 500×500×400 pixels^3. Each B-scan used for 3D-reconstruction was produced and displayed in real-time, every 50 ms. The whole 3D data set was acquired in 2.5 s and a volumetric image immediately displayed. The images were obtained using EXR9.

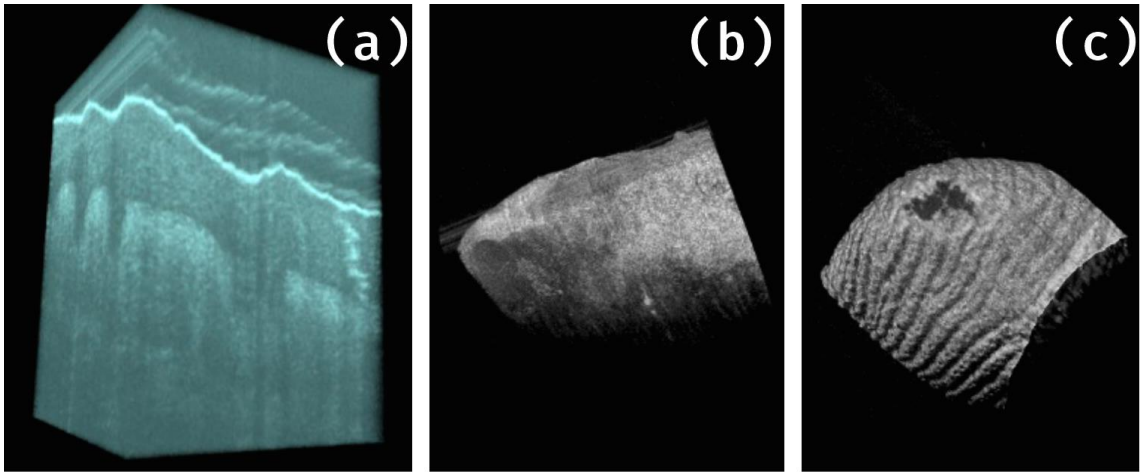

Figure 5: Examples of OCT volumetric images obtained using the EXR9 SC (a) human thumb; (b) human tooth; (c) human finger. All B-scan images were displayed in real-time. Some artifacts due to involuntary movements are visible in each of the 3 images.

In Fig. 6(a) an *en-face* PA image of an USAF target is presented. The smallest elements which c an be separated on this target belong to group 6, element 2. This corresponds to a lateral resolution in the PA channel of 6 µm. Due to the illumination/signal collection geometry, the VIS photons from the COMPACT can eventually hit the transducer itself, so it is very likely that the transducer itself appears in the *en-face* images. This is quite clearly observed in both, Fig. 6(a) and 6(b). To produce the images of the USAF target and human hair, a spectral range of 50 nm around the central wavelength 550 nm was employed.

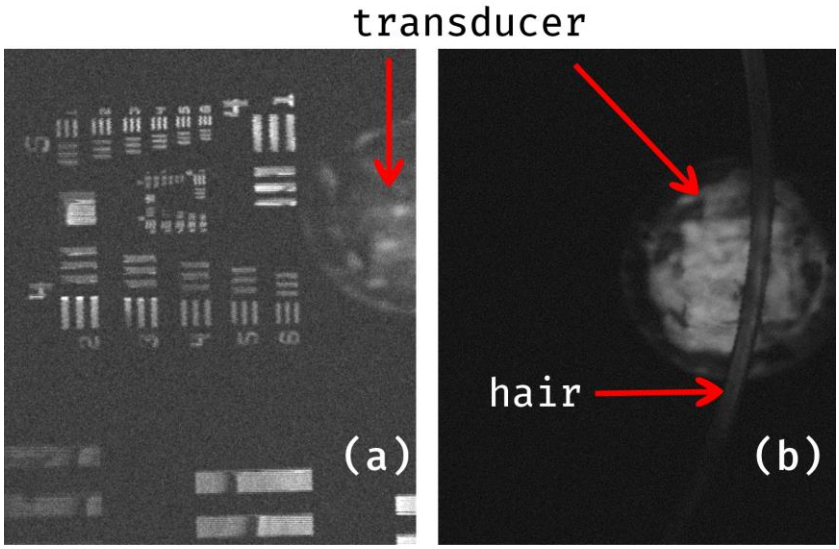

Figure 6: Illustration of the capability of the instrument to produce high resolution PA images. (a) *en-face* PA image of a positive USAF target showing that a lateral resolution as good as 6 µm can be achieved; (b) *en-face* view of the human hair. Due to the illumination geometry the transducer itself can produce ultrasonic waves, hence it appears in the images.

4. ACKNOWLEDGMENTS

G.N. acknowledges the University of Kent for the financial support. A.B. and A.P. acknowledge EPSRC (REBOT grant, EP/N019229/1). A.P. also acknowledges NIHR Biomed. Research Centre at Moorfields Eye Hospital NHS Foundation Trust, the UCL Institute of Ophthalmology, University College London, and the Royal Society Wolfson research merit award.

REFERENCES

[1] Huang, D., Swanson, E. A., Lin, C. P., Schuman, J. S., Stinson, W. G., Chang, W., Hee, M. R., Flotte, T., Gregory, K., Puliafito, C. A., and Fujimoto, J. G., "Optical coherence tomography," Science 254, 1178–1181 (1991).

[2] Andreev, V. G., Karabutov, A. A., Solomatin, S. V., Savateeva, E. V., Aleinikov, Zhulina, et al., "Optoacoustic tomography of breast cancer with arc-array transducer," Proc. SPIE 3916, 36–47 (2000).

[3] Weidner, N., Semple, J. P., Welch, W. R., and Folkman, J., "Tumor angiogenesis and metastasis--correlation in invasive breast carcinoma," N. Engl. J. Med. 324(1), 1–8 (1991).

[4] Bondu, M., Marques, M., Moselund, P. Lall, G., Bradu, A., and A. Podoleanu, "Multispectral photoacoustic microscopy and OCT using a single supercontinuum source," Photoacoustics 9, 21-30 (2018).

[5] Bradu, A. Israelsen, N., Maria, M., Marques, M., Rivet, S., Feuchter, T., Bang, O. and Podoleanu, A., "Recovering distance information in spectral domain interferometry," Scientific Reports 8, 15445 (2018).

[6] Rivet, S., Maria, M., Bradu, A., Feuchter, T., Leick, L., and Podoleanu, A., "Complex master slave interferometry," Opt. Express 24, 2885-2904 (2016).